EXTRACTING ELECTRON ENERGY DISTRIBUTIONS FROM PFRC X-RAY SPECTRA:
PREPARING FOR HIGH-POWER, HIGH-FIELD OPERATION OF THE ROTATING MAGNETIC FIELD

Presentation to the US-Japan CT Workshop

August 24, 2016

Charles Swanson[1], Peter Jandovitz[1], Alexandra Bosh[2], Alexander Glasser[1], Samuel Cohen[1]

[1]Princeton Plasma Physics Laboratory

[2]Virginia Polytechnic Institute and State University

Overview

- The PFRC
  - Seed Plasma
  - RMF-induced plasma
- Novel spectral inversion method
  - Bremsstrahlung
  - The math
  - Calibration using gas-target x-ray tube
- Seed plasma results and discussion
- RMF plasma results and discussion

The PFRC

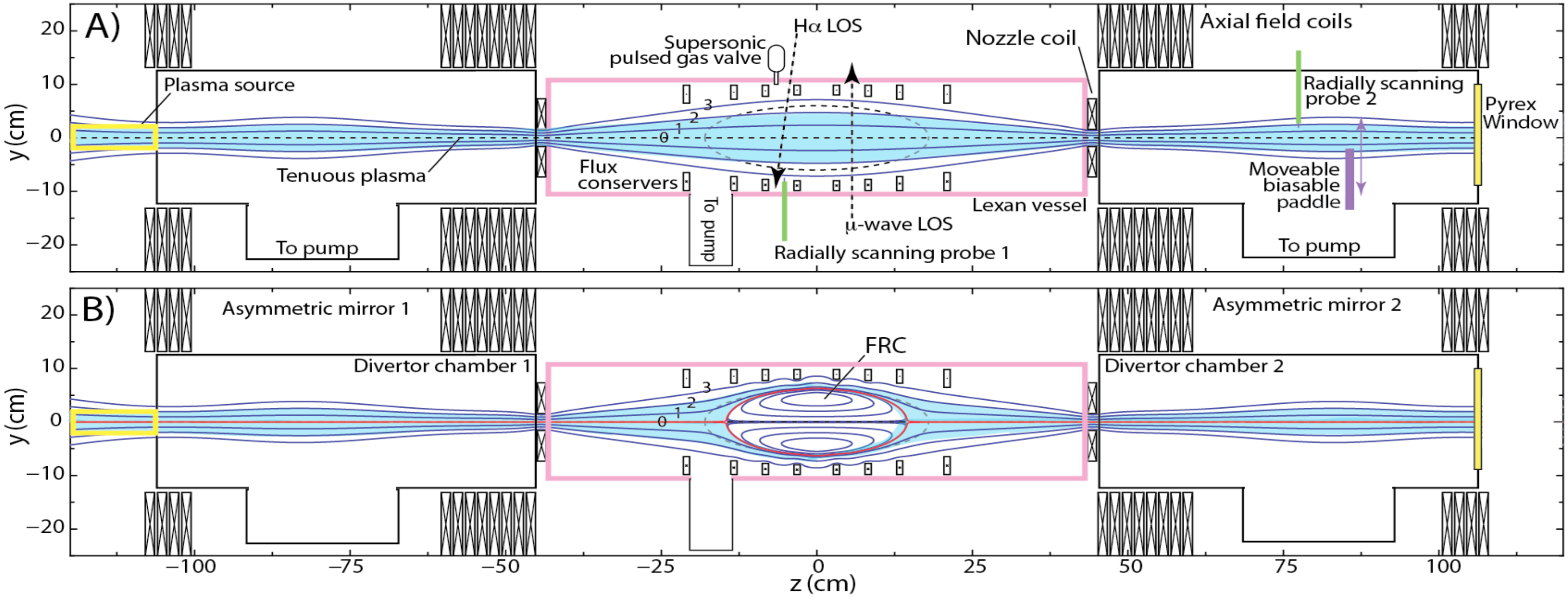

The PFRC-2: magnetic profiles

- The PFRC is a long-pulse, collisionless, low s-parameter experiment to form FRCs using odd-parity rotating magnetic fields.
- Starting with a capacitively-coupled seed plasma (~1-500W), odd-parity rotating magnetic field (RMF) antennae drive current and heat electrons at 10-20kW. An FRC is formed within 200μs. RMF operation continues for 5-250ms.
- Upgrades coming in the next week/month will increase power 10X

Seed Plasma

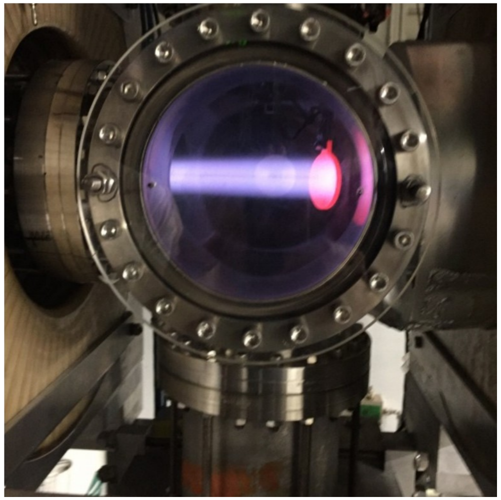

The seed plasma in the Far End Cell strikes a floating plate and causes it to glow red-hot

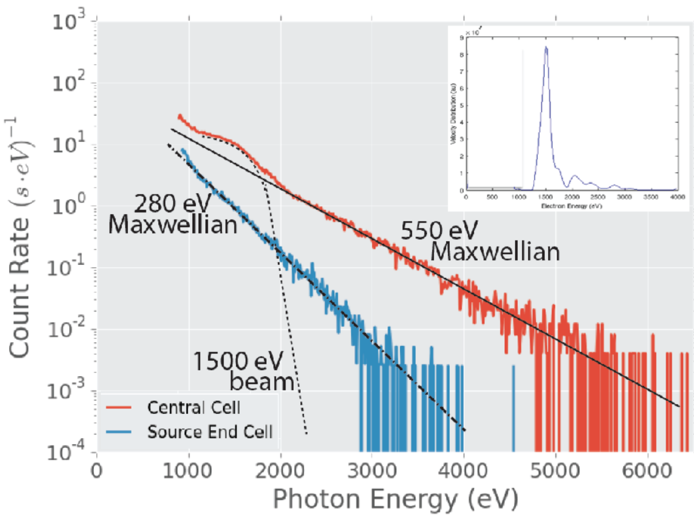

Paper pending by Jandovitz et. al.

- When on, produced by 5 to 500W of capacitively-coupled RF power at the far-left of the machine, 27MHz frequency
- A few $10^{10}/cm^3$, T_e~5eV, yet *see x-rays out to 7keV!*
- **Why would a non-Maxwellian seed plasma be interesting?**
- How do hot electrons affect RMF coupling/penetration?
- Can we use it as a diagnostic?
- How are hot electrons formed and heated, beam and thermal?

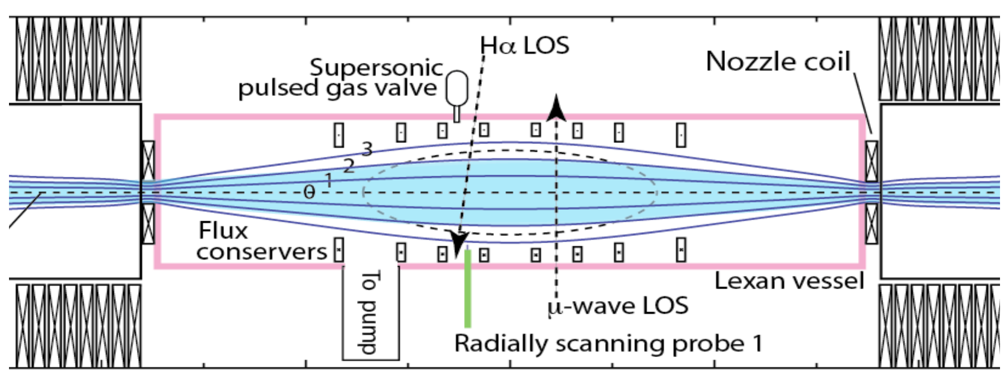

Magnetic configuration during seed plasma operation

RMF Plasma

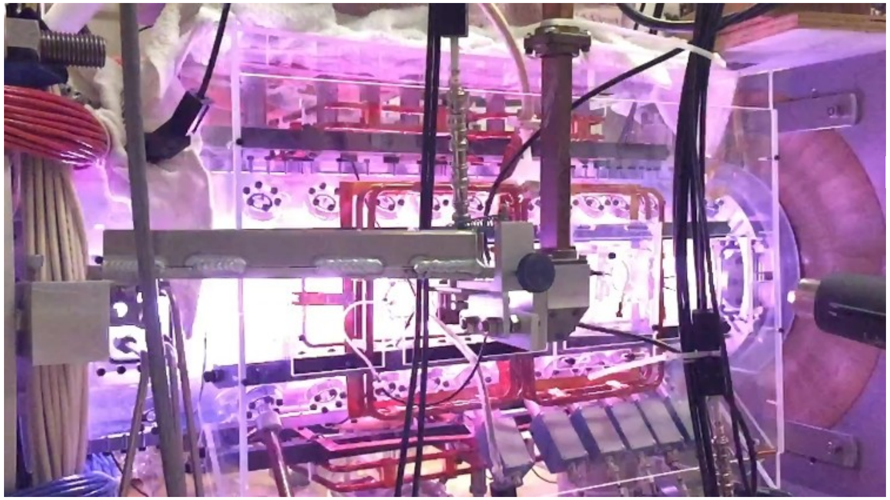

A plasma discharge in the PFRC-2 device

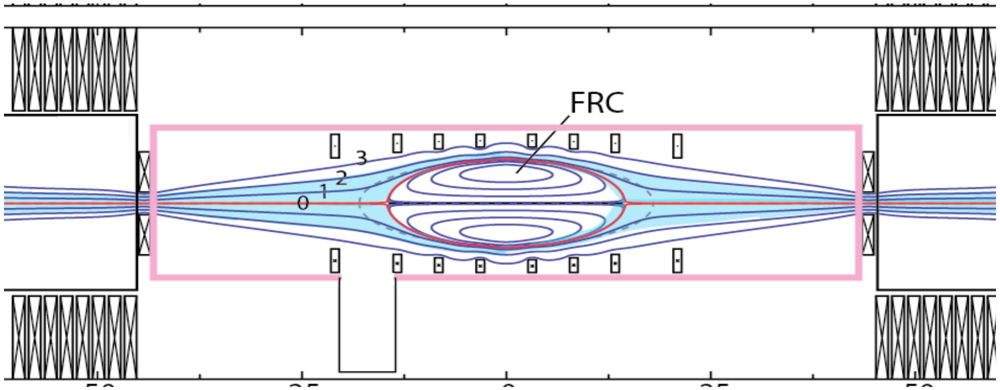

Magnetic configuration during RMF operation

- Produced by up to 20kW (200kW) of RMF power from odd-parity antennae
- 8MHz frequency
- Density a few $10^{12}/cm^3$
- Temperature may be as high as 300eV

RMF Plasma

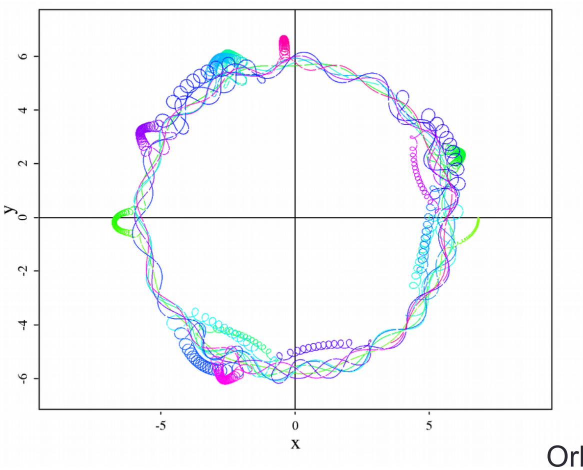

A punctuated betatron orbit

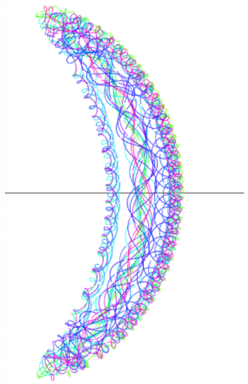

Orbit in the co-rotating frame illustrating trapping

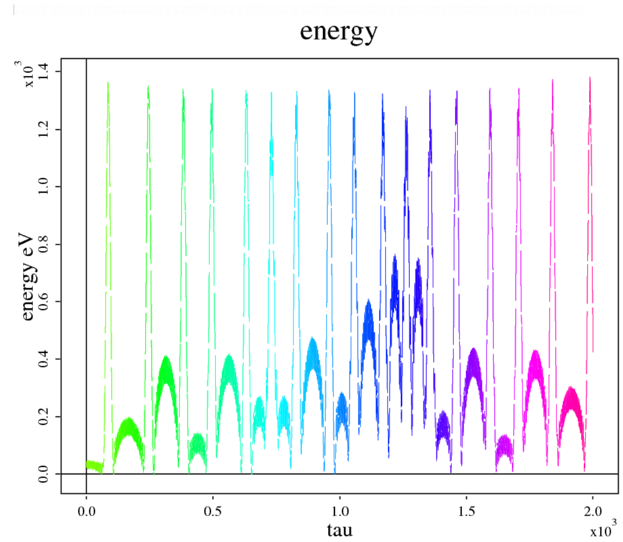

Time-history of energy of a particle in the PFRC-2 from a single-particle motion code

- **Why would a non-Maxwellian RMF plasma be interesting?**
  - Our heating mechanism has an inductive $\vec{E}$ that traps and accelerates particles along the magnetic null.
  - Single-particle codes predict our heating mechanism to produce non-thermal distribution, have a hard cutoff
  - Need turbulence to heat past the cutoff and equilibrate to thermal: Lower Hybrid Drift mode.

PFRC-1 device saw a Maxwellian tail with density ~10^12 and temperature ~200eV

RMF: What do we *expect?*

- More on the RMF_o heating mechanism: Single-particle motion Hamiltonian simulation results

Maximum energy is constrained

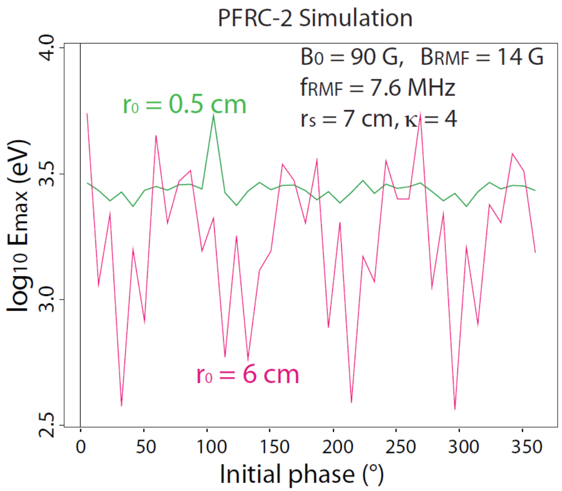

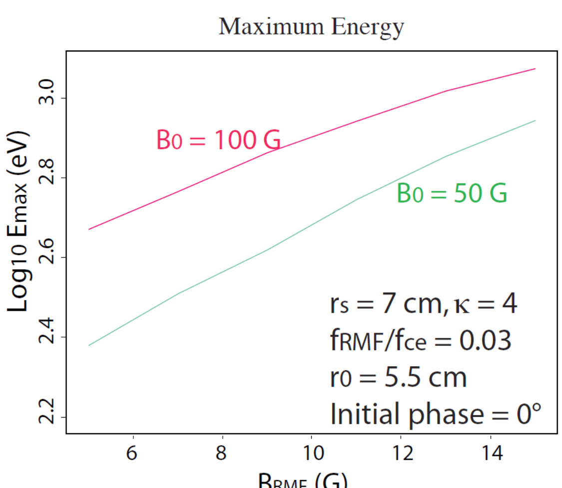

Average energy is of the same order (~0.3)

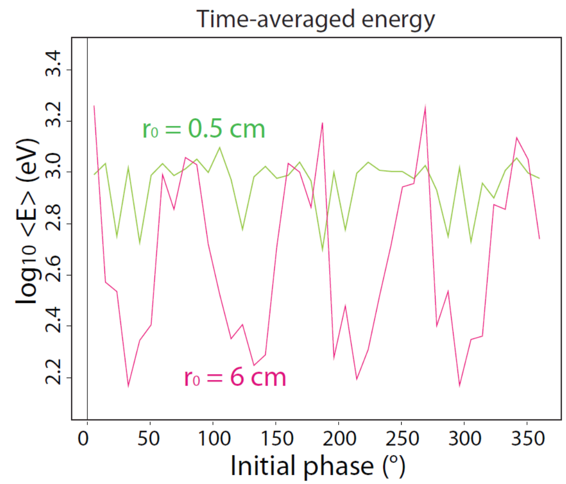

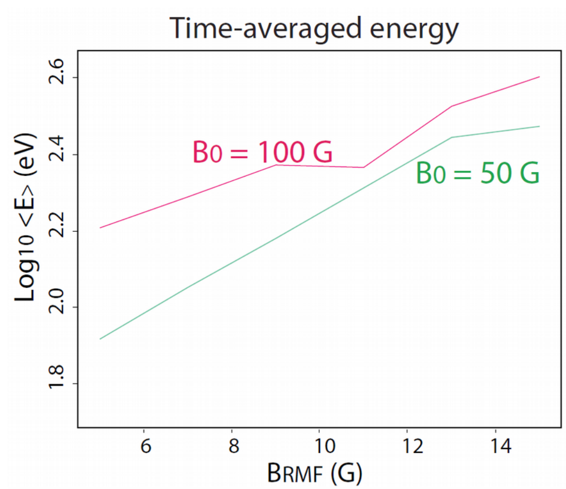

Example distribution of energies: Non Maxwellian, truncated

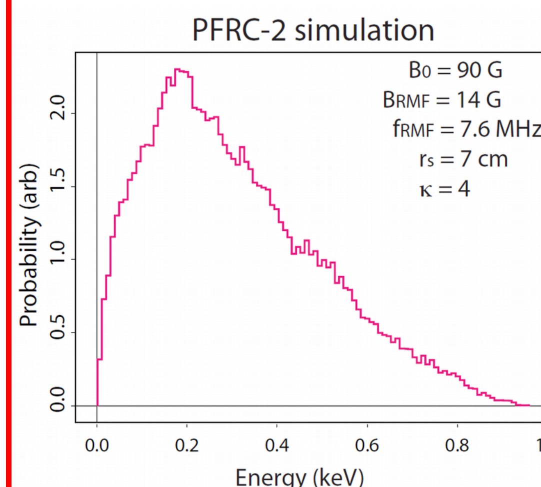

X-Ray Detectors

http://amptek.com/

We have Amptek Si-PIN diode detectors. They detect x-rays, determine their energy with some accuracy, and count the number within each *energy channel*.
Have low-energy limit on detected x-rays: 600eV-1keV

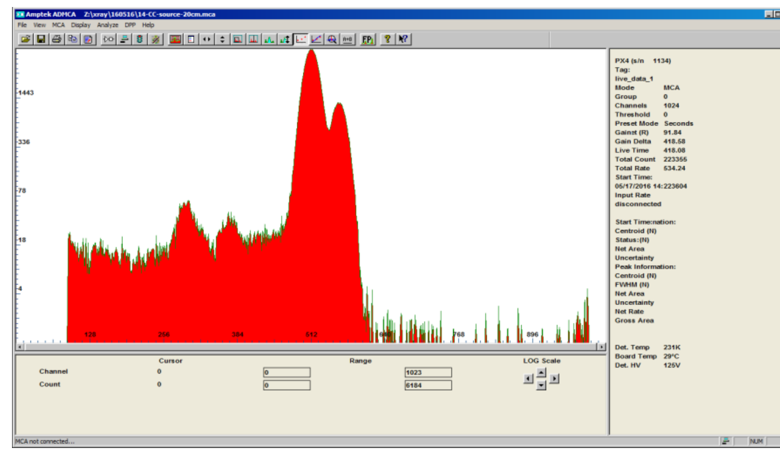

Example spectrum (Fe-55)
2016/05/16

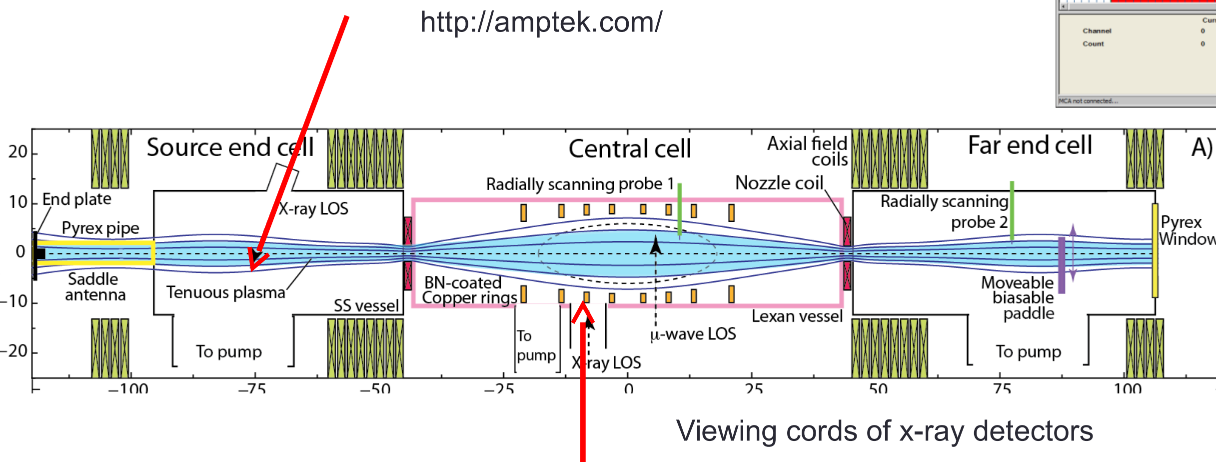

Viewing cords of x-ray detectors

Overview

- ~~The PFRC~~
  - ~~Seed Plasma~~
  - ~~RMF-induced plasma~~
- Novel spectral inversion method
  - Bremsstrahlung
  - The math
  - Calibration using gas-target x-ray tube
- Seed plasma results and discussion
- RMF plasma results and discussion

Bremsstrahlung

- Electrons in the vicinity of nuclei accelerate and emit EM radiation. The differential cross section to emit an x-ray between ν and $\nu + d\nu$ is given by the equation

$$I(\nu) = r_e^3 \frac{m_e c^2 32\pi^2}{h3\sqrt{3}} \int d\beta \frac{f(\beta)G(\beta,\nu)}{\beta\nu}$$

- Or in energy units

$$I(E_x) = K \int dE_x \frac{f(E_e)G(E_x, E_e)}{E_x\sqrt{E_e}}$$

Where E_x is the energy of the x-ray, E_e is the energy of the electron, G is the "Gaunt factor."

- When discretized, this is a matrix multiplication:

$$\overrightarrow{I_{x,i}} = \sum_j M_{i,j}\overrightarrow{I_{e,j}} = \left(M\overrightarrow{I_e}\right)_i$$

Where $M_{i,j} = KG(E_{x,i}, E_{e,j})/E_{x,i}\sqrt{E_{e,j}}$

- **Spectral lines are not considered**

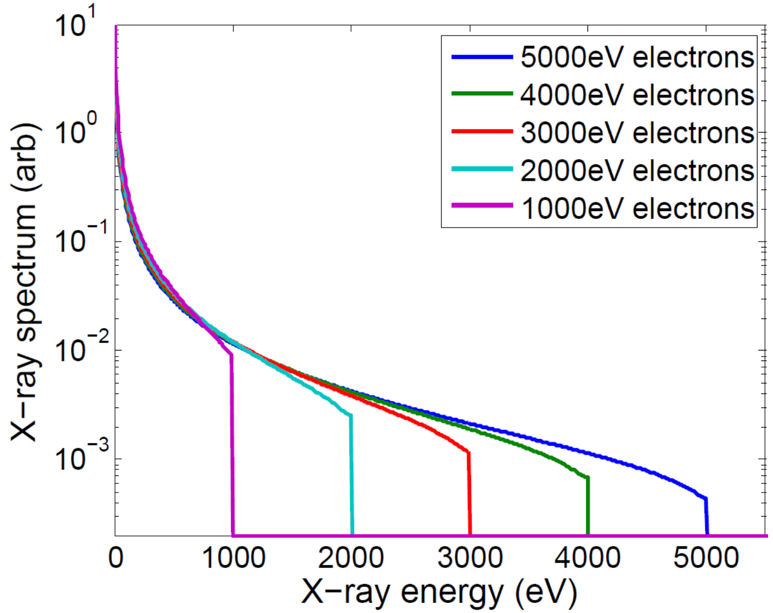

$I(E_x)$ produced by delta-functions of $f(E_e)$

Spectral Inversion

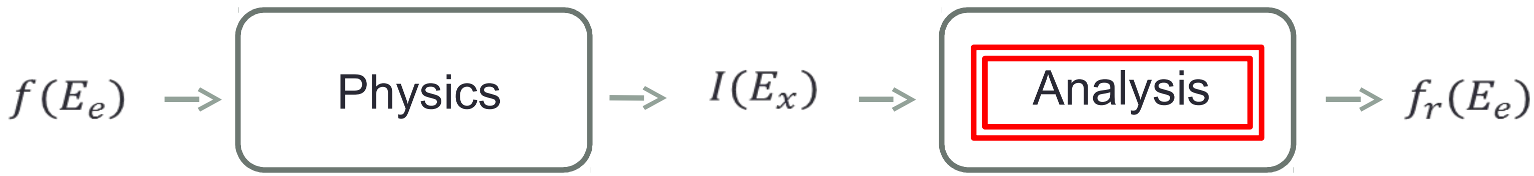

- Matrix Inversion. $M^{-1}I_x = M^{-1}MI_e = I_e$. This method is *unstable to numerical noise*. It yields *unphysical results.*

- Instead let us *maximize the log-likelihood* that our model ($f(E_e)$) produces our data ($I(E_x)$).
  - Maximizing the log-likelihood comes from Bayes's Theorem; it's the formally consistent way to do statistical inference.

  - Minimize the log-likelihood with respect to our model variables, in this case $\{I_e\}$ values. Find the $\overrightarrow{I_e}$ that minimizes this quantity.

  - An example of this is Tikhonov Regularization [2][3], in which the quantity $||MI_e - I_x||^2 - \lambda||I_e||^2$ is minimized, the log-likelihood for Gaussian measurements. $||Q||$ is the Euclidean norm of quantity Q.

Poisson Regularization

X-ray counts in each channel is a Poisson distributed random variable. Poisson Distribution:

$$P(a|b) = \frac{b^a e^{-b}}{a!}$$

Thus we minimize the log-likelihood:
$\ln[P(b|a)P(a)]$ is…

$$\text{minimize} \sum MI_e - I_x \ln(MI_e) + [\ln \sum I_e] + etc$$

prior

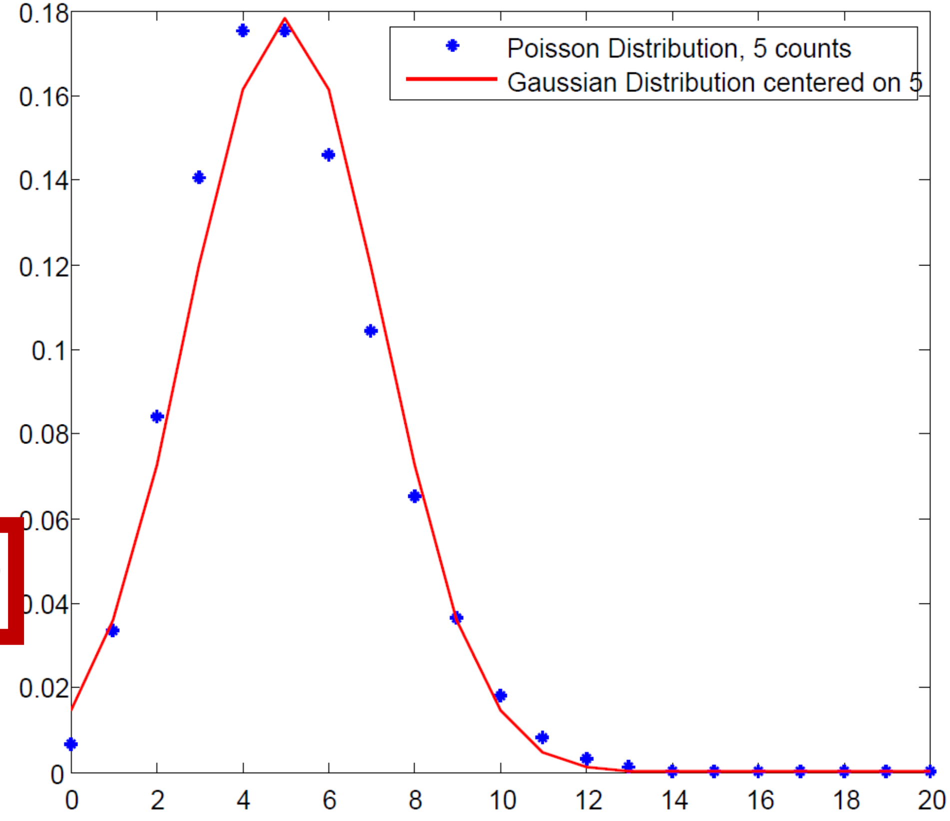

That quantity is a function of N independent variables, $\{I_e\}$. We use a quasi-Newton method to optimize, but there are many usable algorithms to optimize a high-dimensional problem.

Choice of $M_{i,j}$

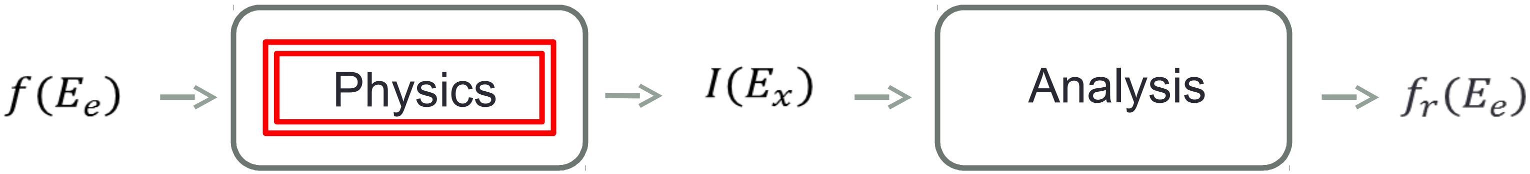

We can go even farther. In our matrix we can include the effects of the transmission efficiency and finite resolution.

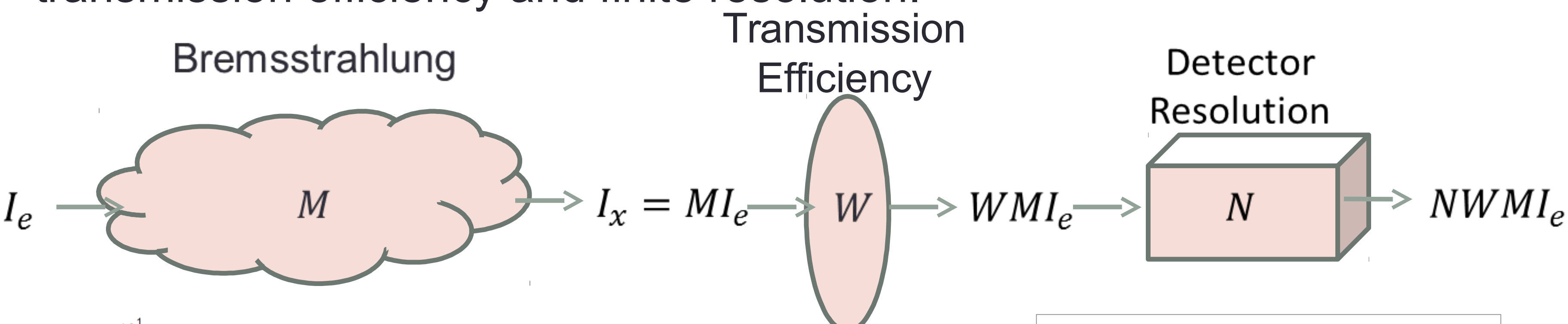

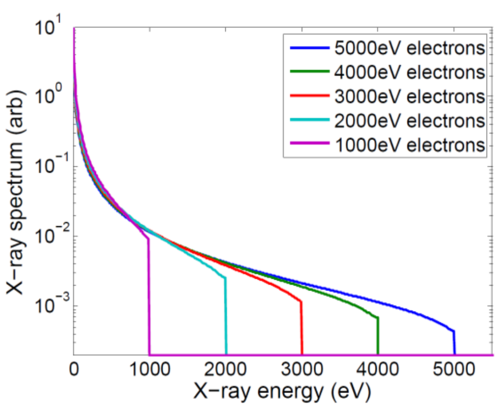

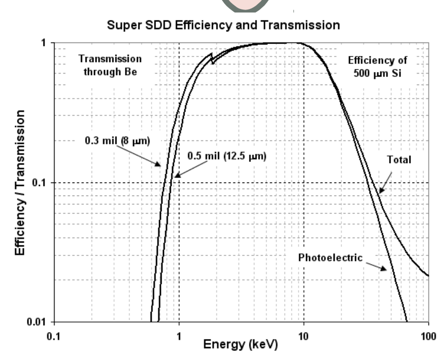

http://amptek.com/

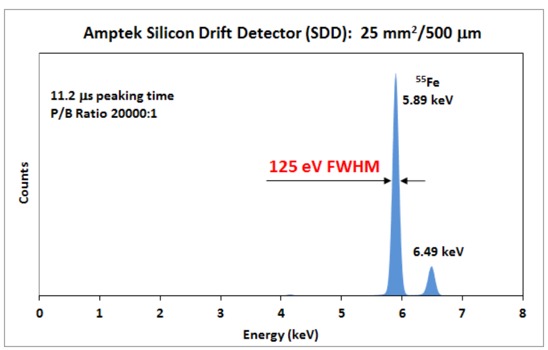

http://amptek.com/

Calibration

- We can even directly measure $M_{i,j}$ using gas-target Bremsstrahlung in an x-ray tube.

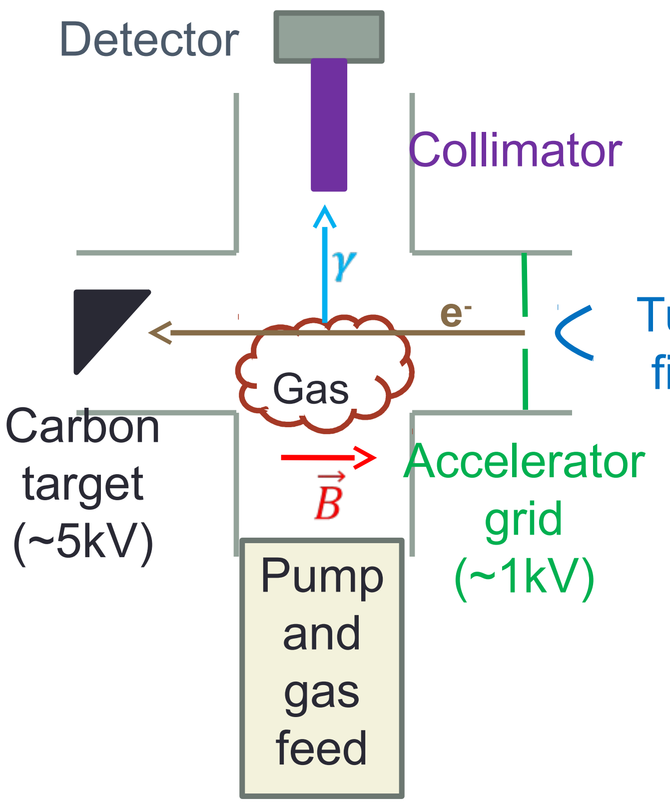

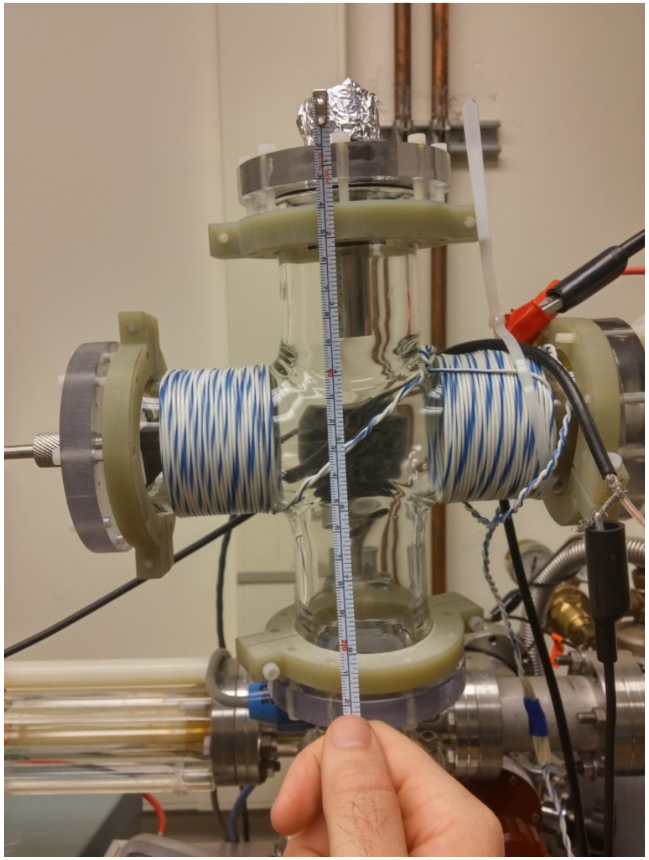

- We also use radioactive sources

Anatomy of an Inverted Spectrum

- In the x-ray tube, neon gas fill, 3600eV beam energy
- Using the Elwert approximation to the Gaunt factor: Spectral lines not included, produce artificial spikes in spectrum. This is not the case of calibrated analysis.

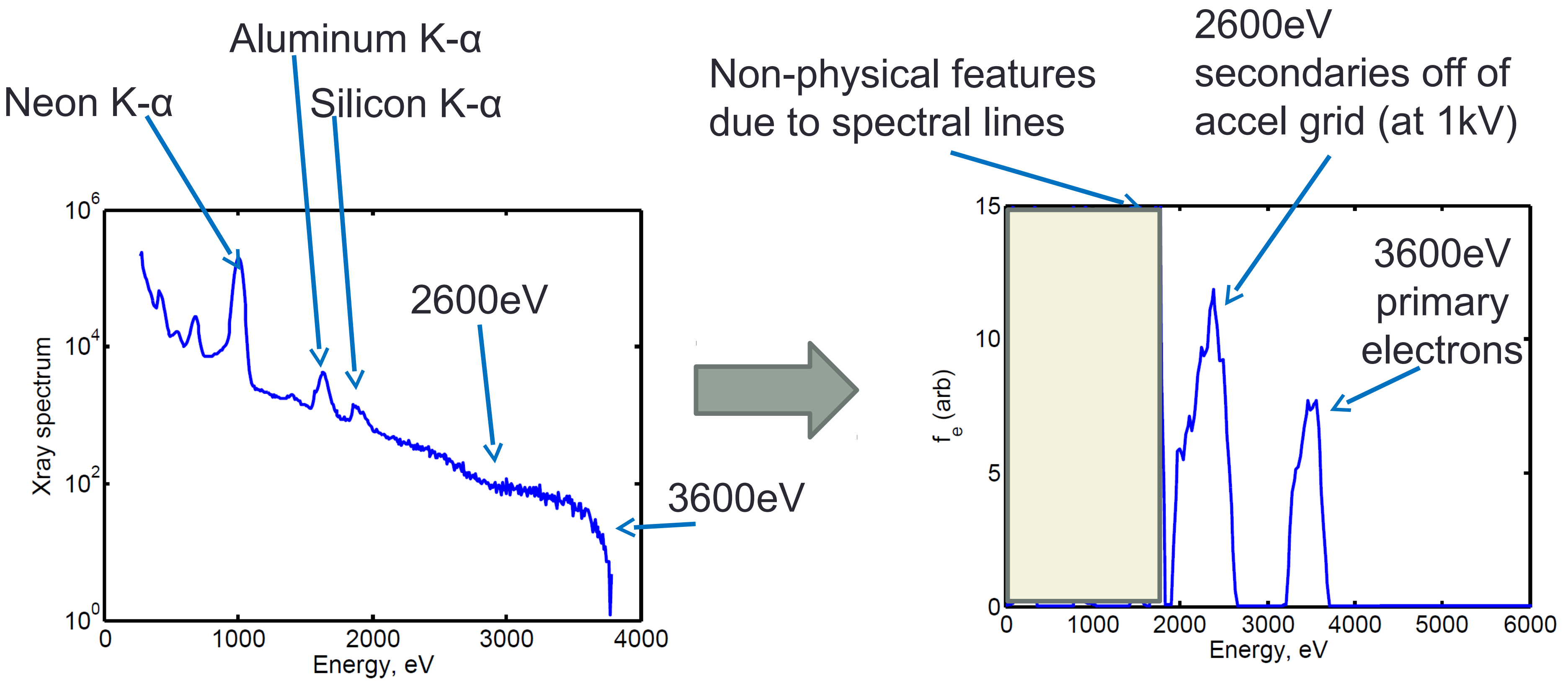

Corrected x-ray spectrum
2016/08/15

Inverted electron spectrum
2016/08/15

Anatomy of an Inverted Spectrum

- In the x-ray tube, neon gas fill, 3600eV beam energy
- Using the Elwert approximation to the Gaunt factor: Spectral lines not included, produce artificial spikes in spectrum. This is not the case of calibrated analysis.

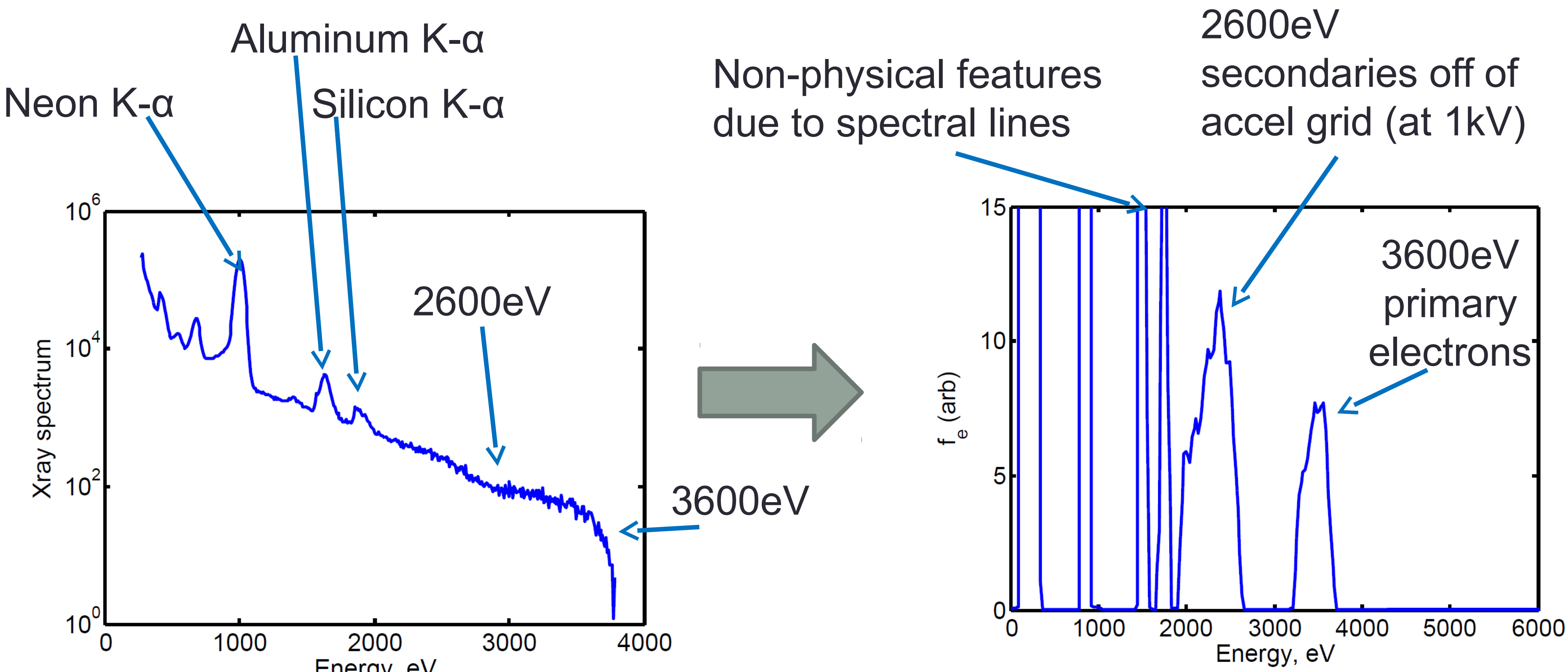

Corrected x-ray spectrum 2016/08/15

Inverted electron spectrum 2016/08/15

Spectrum Inversion to find spectral lines

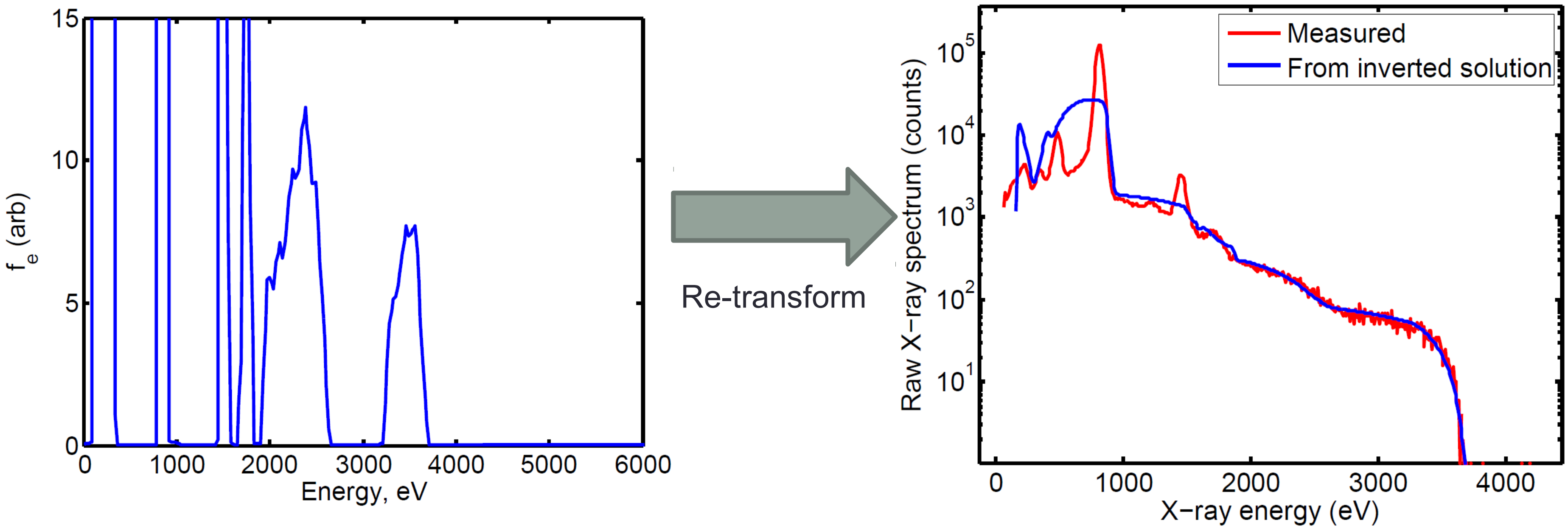

- Spectral lines are not considered by the previous slide's analysis; produce incorrect electron distributions.
- Re-transforming these electron distributions back into x-ray distributions yield discrepancies.
- *No* plasma could have produced the measured x-ray spectrum via only Bremsstrahlung. Spectral lines are *required* to produce those peaks.

Overview

- ~~The PFRC~~
  - ~~Seed Plasma~~
  - ~~RMF-induced plasma~~
- ~~Novel spectral inversion method~~
  - ~~Bremsstrahlung~~
  - ~~The math~~
  - ~~Calibration using gas-target x-ray tube~~
- Seed plasma results and discussion
- RMF plasma results and discussion

Seed Plasma Results: High power H_2

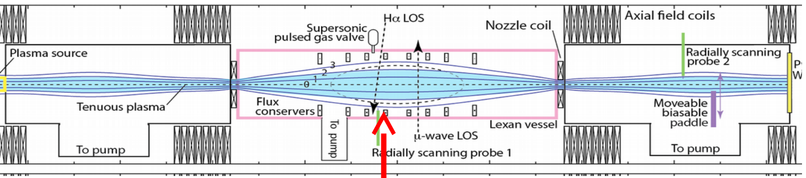

- Center Cell, **400W** RF power, H_2 gas

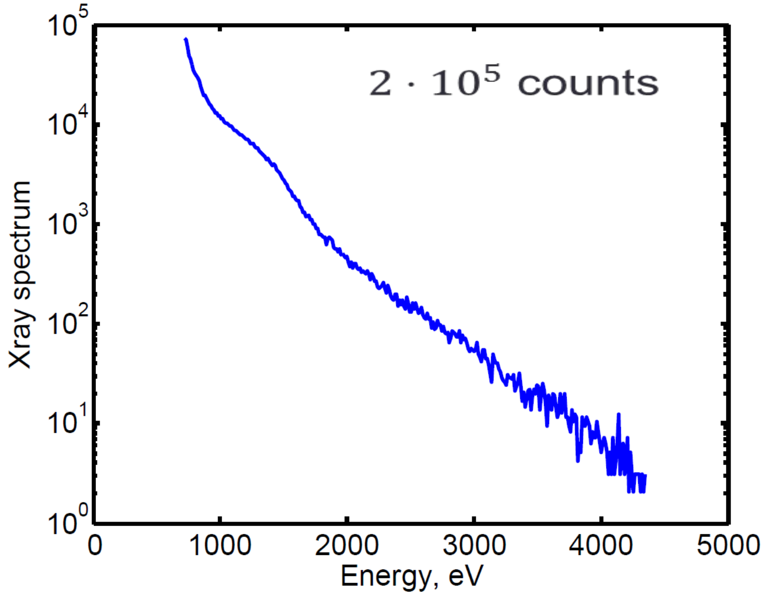

Corrected x-ray spectrum
2016/04/13

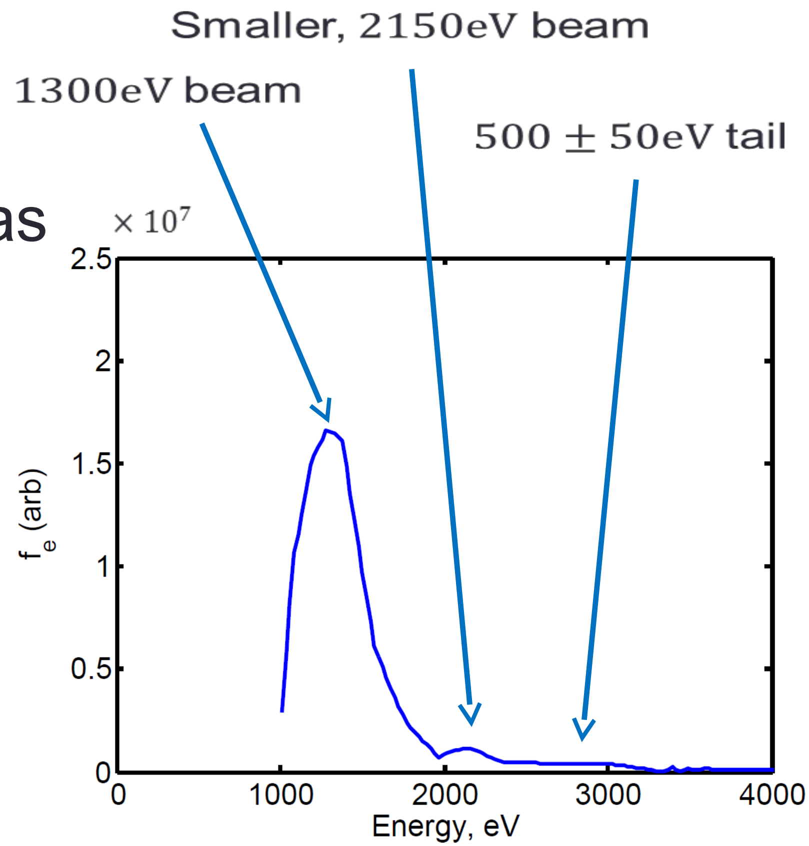

Inverted electron spectrum
2016/04/13

Beam integrates to a density of $1 \cdot 10^8/\mathrm{cm}^3$ of bulk density $\sim 10^{10}/\mathrm{cm}^3$

Seed Plasma Results: High power H_2

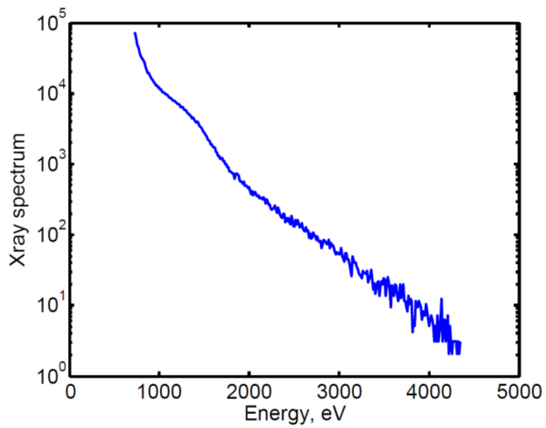

Corrected x-ray spectrum
2016/04/13

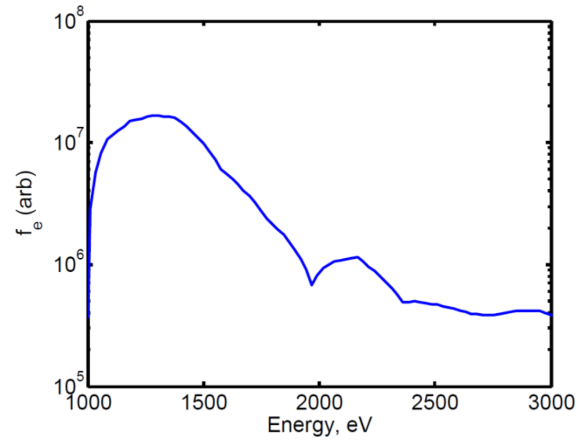

Inverted electron spectrum, log scale
2016/04/13

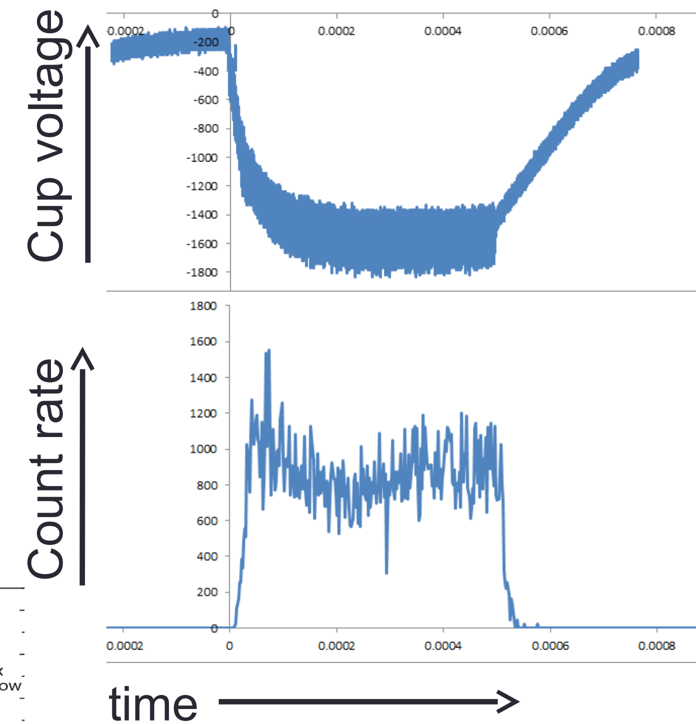

Example comparison between carbon cup voltage and center cell count rate
2016/08/05 and 2016/08/09

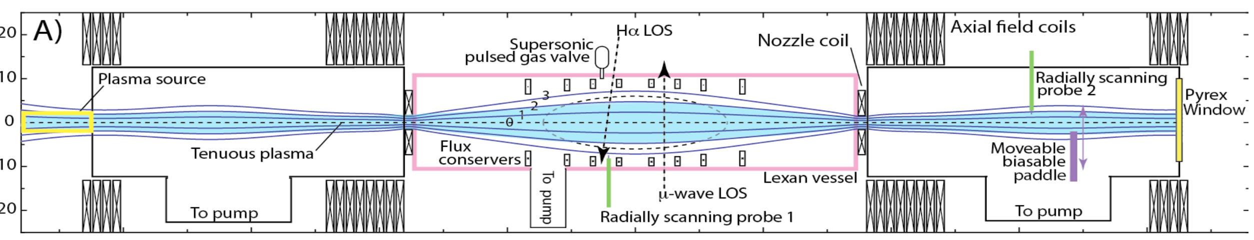

- 1300eV beam: In Source End Cell, plasma terminates on carbon cup (left)
  - This carbon cup floated at -1900V with oscillations of $375V_{pkpk}$
  - Beam has 500eV FWHM
  - Plasma termination paddle at *other* end floats at -600V
- 2150eV beam: Oscillations must heat our beam. Resonances exist.

Seed Plasma Results: Low power H_2

- Center Cell, **100W** RF power, H_2 gas

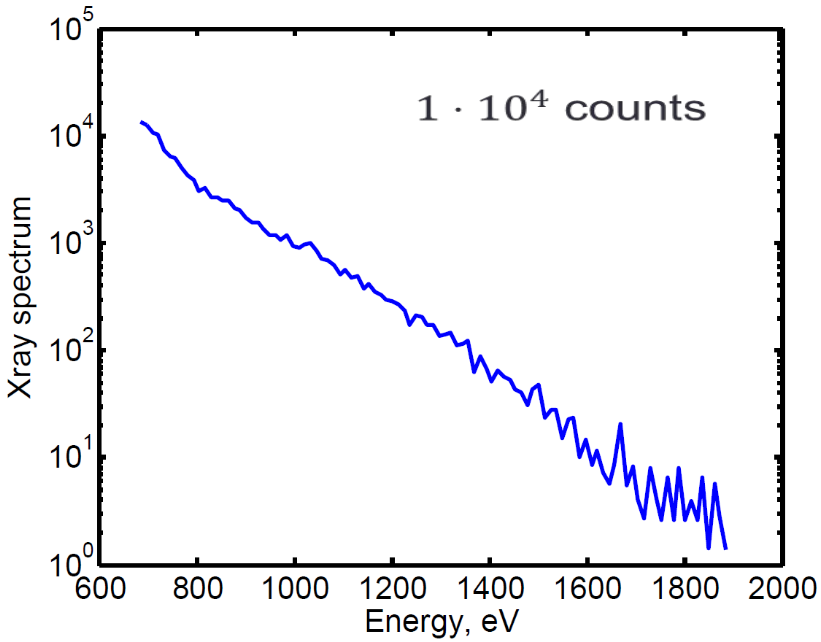

Corrected x-ray spectrum
2016/04/06

140 ± 30eV thermal-like

Beam at 1300eV

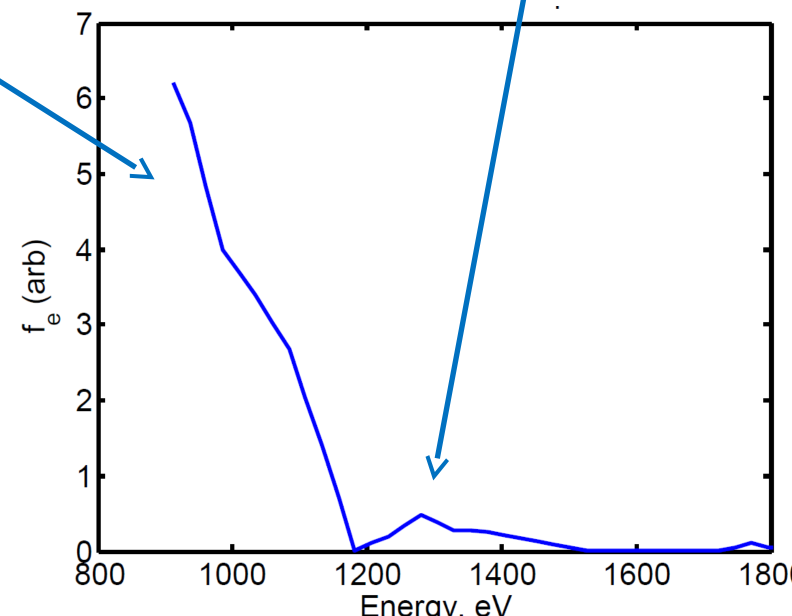

Inverted electron spectrum
2016/04/06

Carbon cup floating potential: -1000V
Far end paddle: ~0V

Beam integrates to a density of $8 \cdot 10^6/\text{cm}^3$ of bulk density $\sim 10^{10}/\text{cm}^3$

Seed Plasma Results: Argon

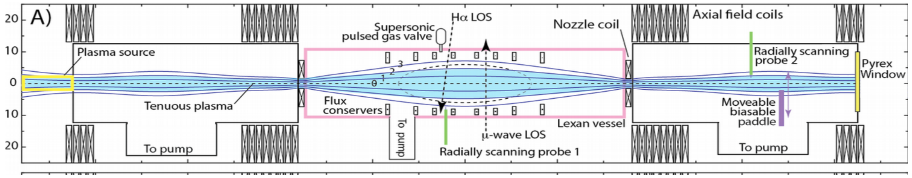

- Source End Cell, **350W** RF power, Ar gas

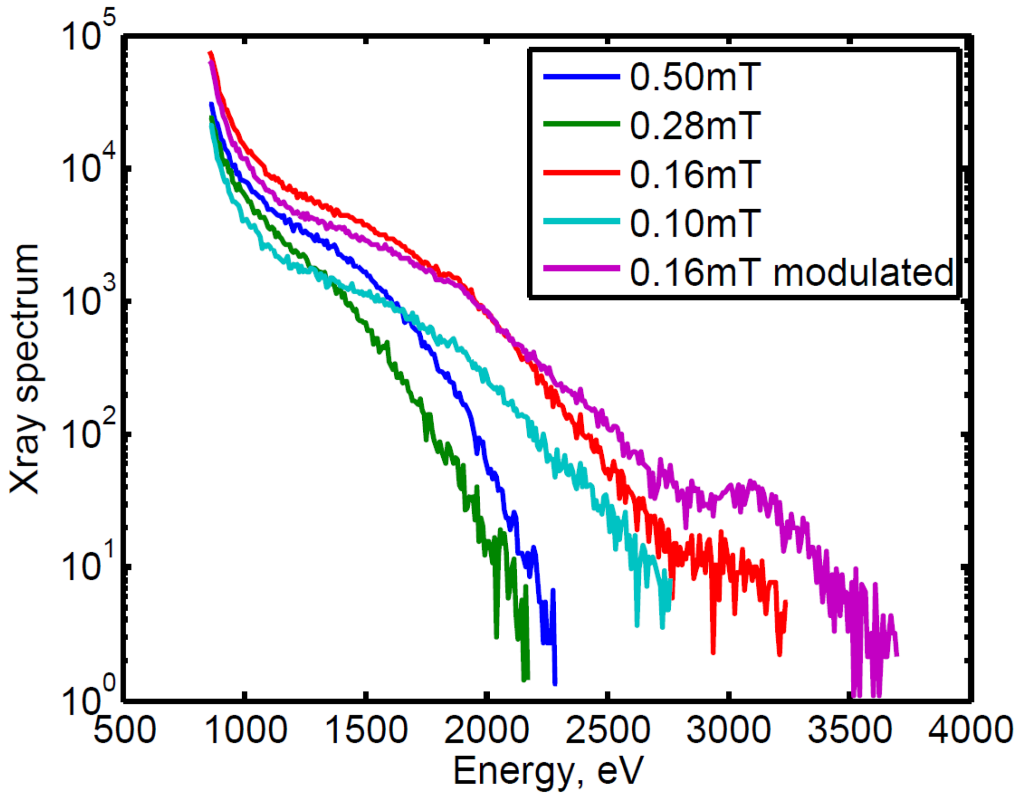

Corrected x-ray spectrum
2016/08/05

Seed Plasma Results: Argon, high pressure

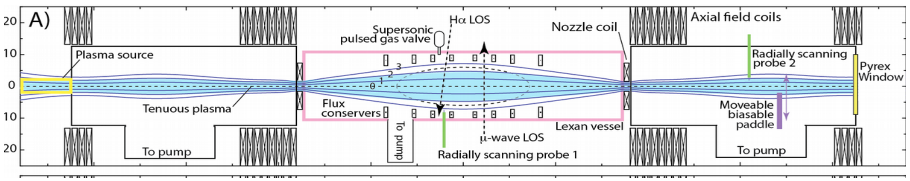

- Source End Cell, **350W** RF power, Ar gas

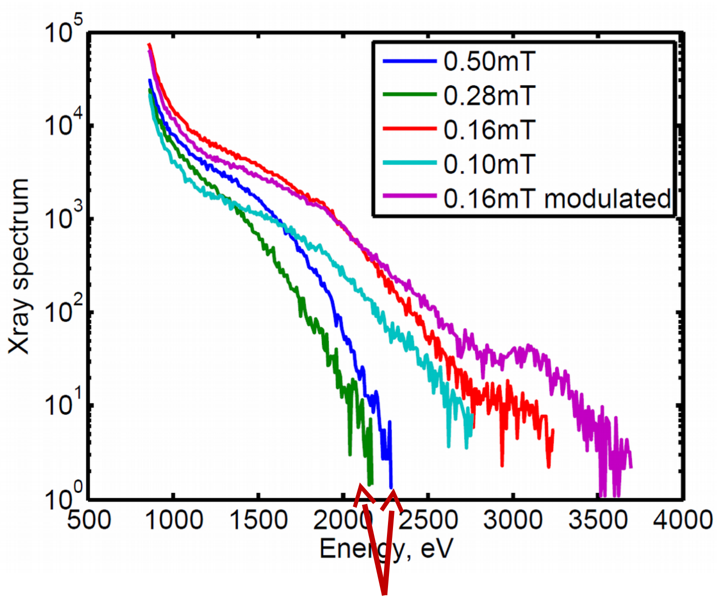

These first two show hard cutoffs in energy

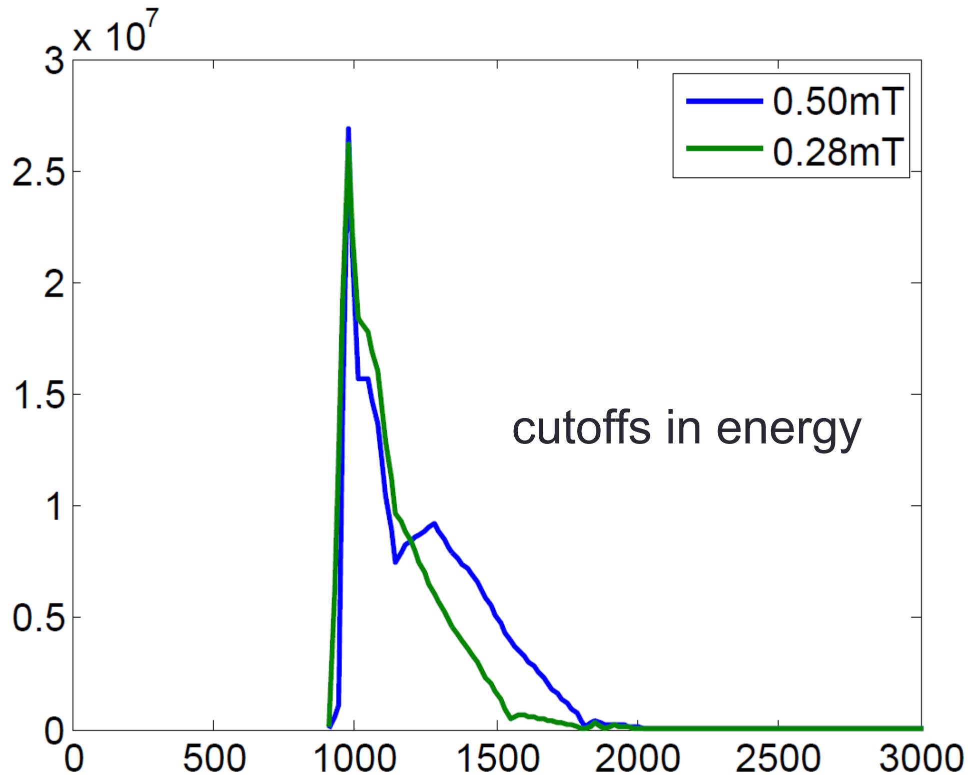

Corrected x-ray spectrum
2016/08/05

Seed Plasma Results: Argon, low pressure

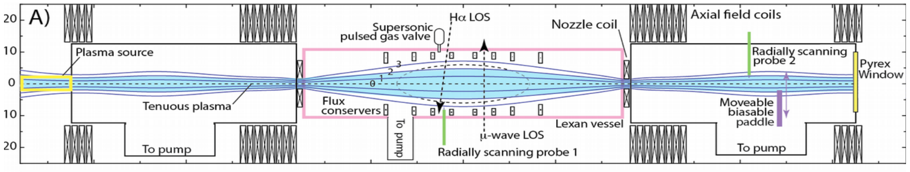

- Source End Cell, **350W** RF power, Ar gas

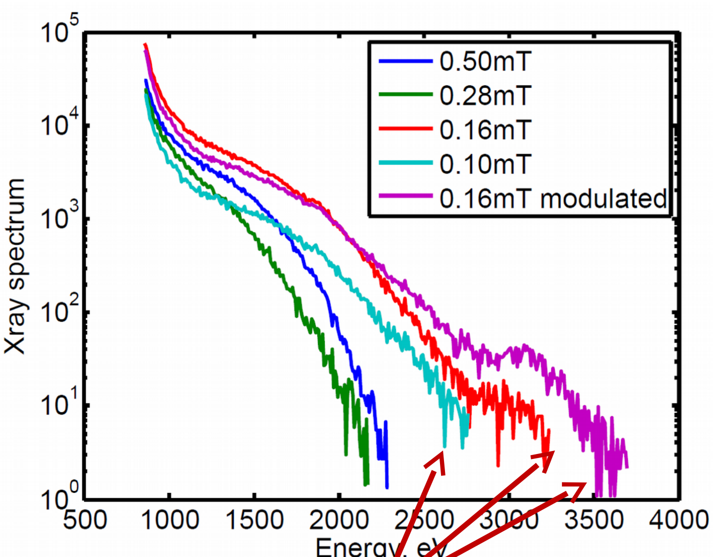

These three have spectral lines visible

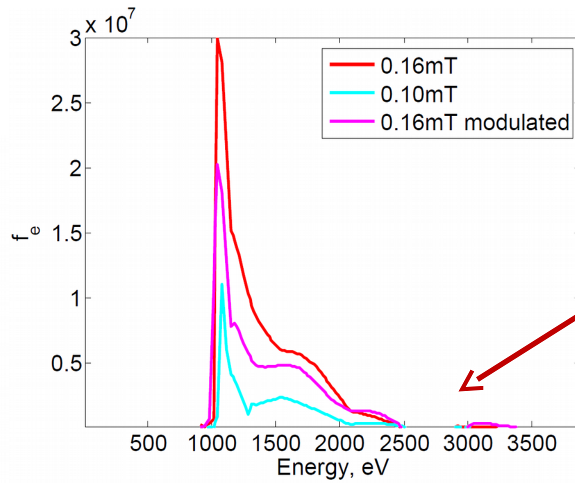

Inverted x-ray spectrum
2016/08/05

Non-physical hollow and peak before and after spectral line

Beam and sub-beam, as with H_2

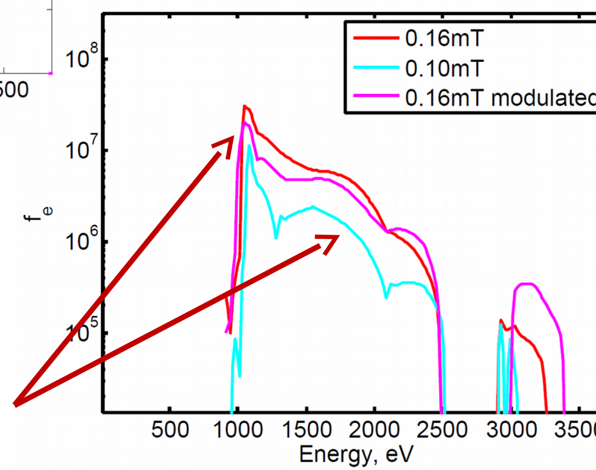

Inverted x-ray spectrum on a log scale
2016/08/05

Seed Plasma Discussion

- The diagnostic can determine features like beams and cutoffs and measure their amplitudes.
- The diagnostic can be used to identify spectral lines

- Fast electrons were never considered in RMF calculation and simulation
  - How do they affect RMF coupling? Penetration?
  - Previous simulation has started with a thermal distribution

RMF Plasma Results

- Center Cell, 13.5kW RMF power, 300W seed power

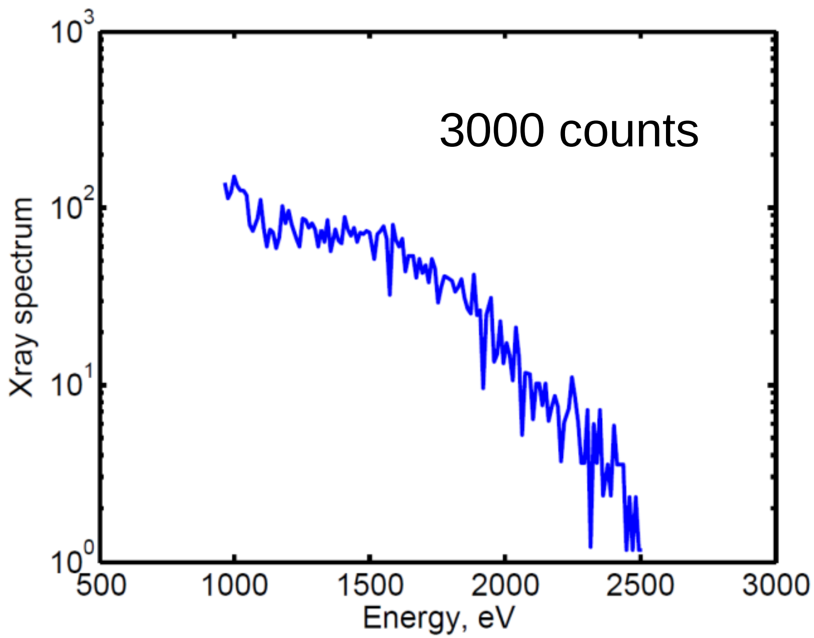

Corrected x-ray spectrum
2015/10/30

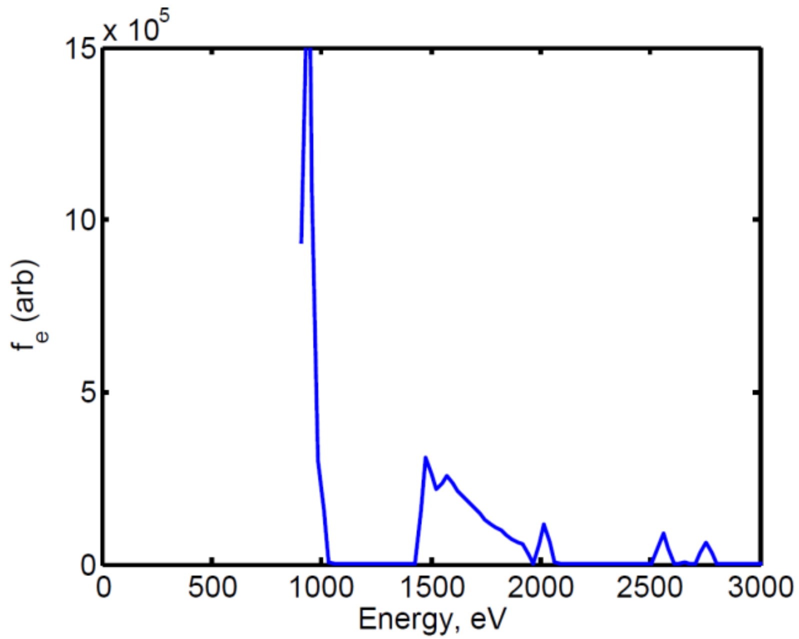

Inverted electron spectrum
2015/10/30

- Unexpectedly low count rate.
- Beam at 1500eV
- $T_e = 250 \pm 50\text{eV}$
- Assuming beam, $n_e = 3 \cdot 10^8/\text{cm}^3$

Reminder: What did we *expect?*

- Single-particle motion Hamiltonian simulation results example distribution

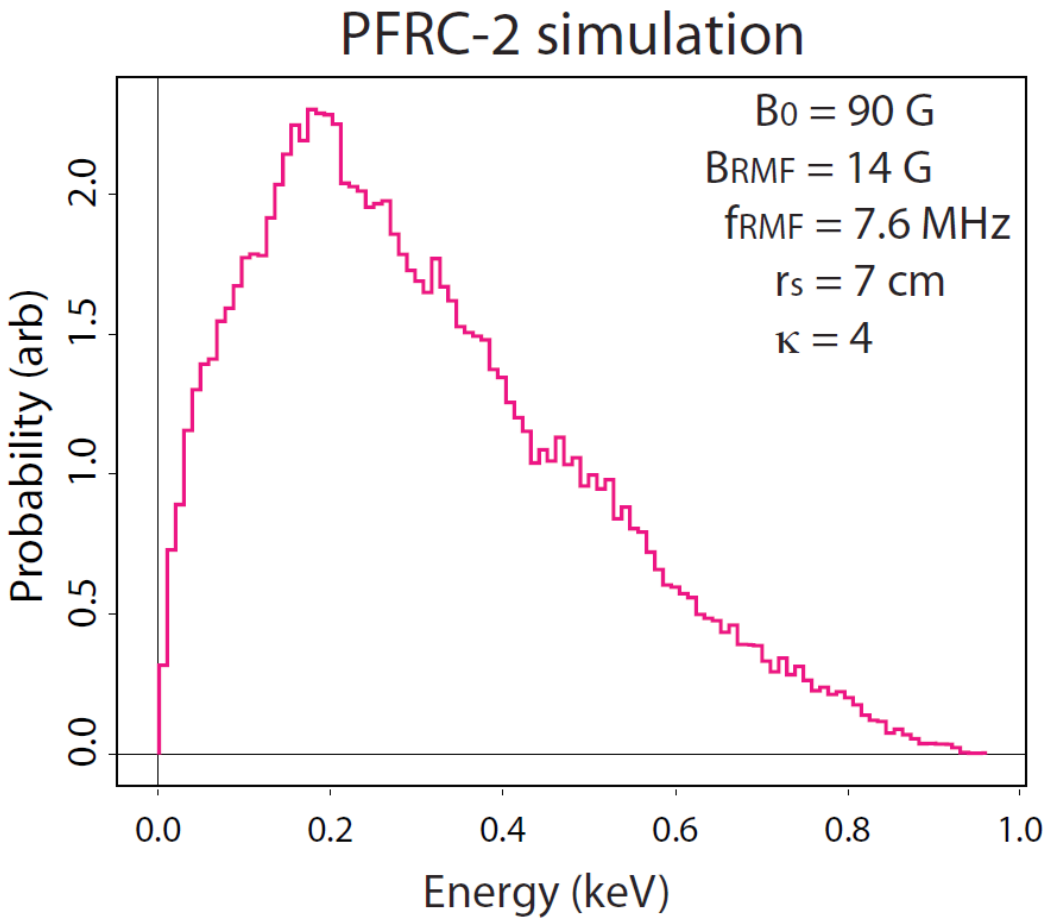

RMF Plasma Results: Seed Comparison

- Center Cell, 13.5kW RMF power, 300W seed power

During RMF Pulse

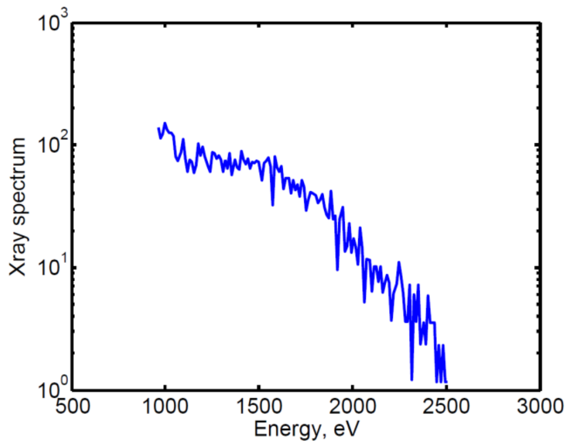

Corrected x-ray spectrum
2015/10/30

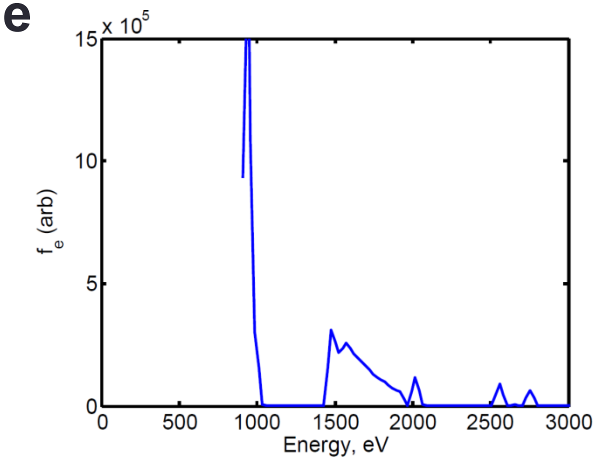

Inverted electron spectrum
2015/10/30

Outside RMF Pulse (seed only)

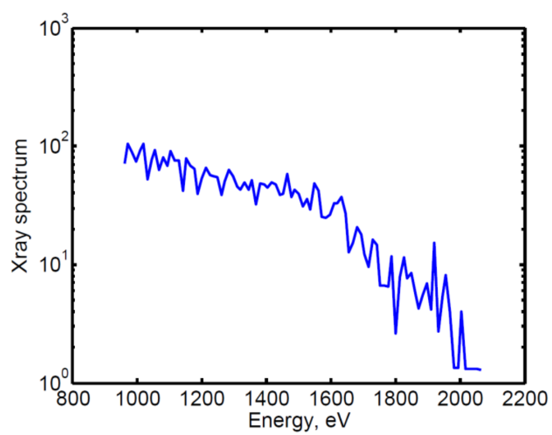

Corrected x-ray spectrum
2015/10/30

Seed count rate ~30X lower

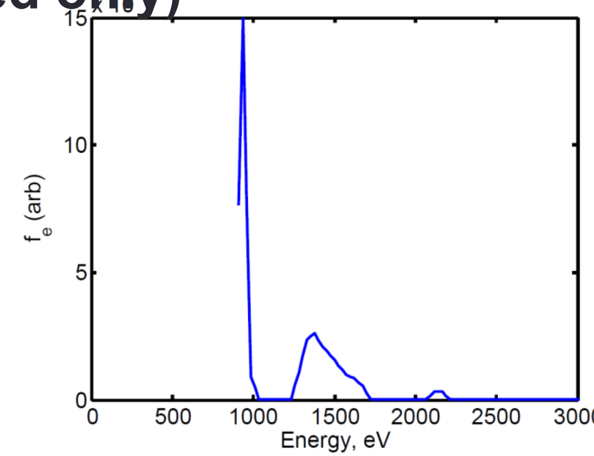

Inverted electron spectrum
2015/10/30

RMF Plasma Results: Low seed

- Center Cell, 19.5kW RMF power, 30W seed power

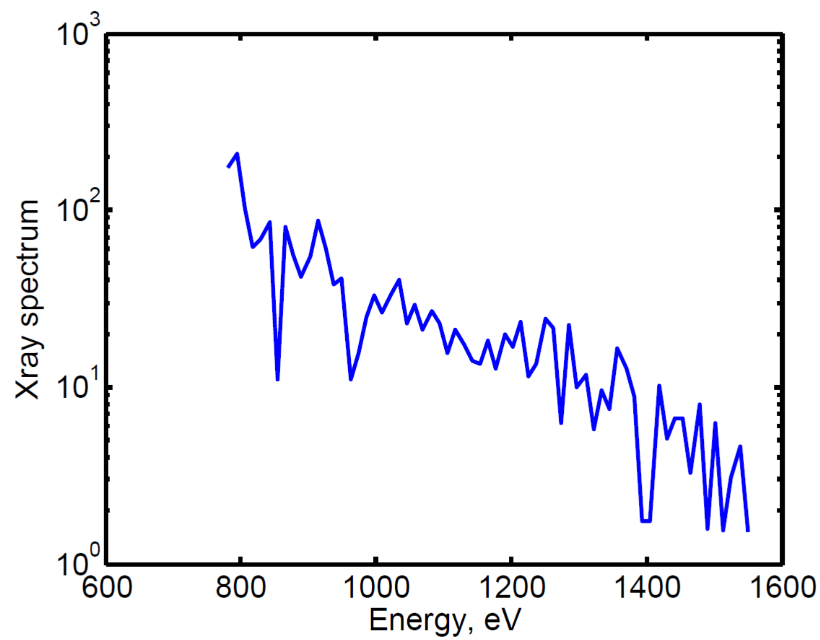

Corrected x-ray spectrum
2016/07/19

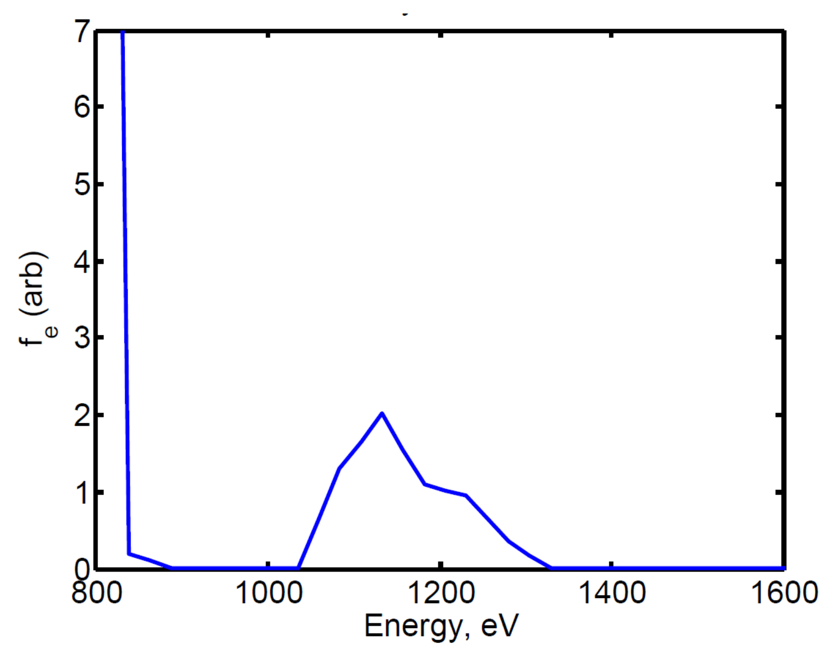

Inverted electron spectrum
2016/07/19

- Beam at 1150eV
- $T_e = 130 \pm 60\text{eV}$
- Assuming thermal, $n_e = 3 \cdot 10^9/\text{cm}^3$
- Assuming beam, $n_e = 3 \cdot 10^7/\text{cm}^3$

RMF Plasma Discussion

- Even if hot electrons are thermal during RMF, only account for 1-3% of electrons
- Clearly interesting physics is happening. Possibilities:
  - Micro turbulence insufficient to equilibrate to thermal
  - RMF heating minority population (seed beam?) preferentially
- This technique will settle these questions
  - Calibrated data will take into account spectral lines, unaccounted-for detector effects
  - New detector can see down to 400eV

Acknowledgements

- Bruce Berlinger, for being a technician
- Eugene Evans, for ideas
- Ken Hill and Manfred Bitter, for practical x-ray expertise

- This work was supported, in part, by DOE Contract Number DE-AC02-09CH11466

Citations

- [1] Cohen, S. A., B. Berlinger, C. Brunkhorst, A. Brooks, N. Ferraro, D. P. Lundberg, A. Roach, and A. H. Glasser. "Formation of Collisionless High- β Plasmas by Odd-Parity Rotating Magnetic Fields." *Physical Review Letters* 98, no. 14 (April 5, 2007). doi:10.1103/PhysRevLett.98.145002.
- [2] Piana, Michele, Anna Maria Massone, Eduard P. Kontar, A. Gordon Emslie, John C. Brown, and Richard A. Schwartz. "Regularized Electron Flux Spectra in the 2002 July 23 Solar Flare." *The Astrophysical Journal* 595, no. 2 (October 1, 2003): L127–30. doi:10.1086/378171.
- [3] Brown, John C., A. Gordon Emslie, Gordon D. Holman, Christopher M. Johns-Krull, Eduard P. Kontar, Robert P. Lin, Anna Maria Massone, and Michele Piana. "Evaluation of Algorithms for Reconstructing Electron Spectra from Their Bremsstrahlung Hard X-Ray Spectra." *The Astrophysical Journal* 643, no. 1 (May 20, 2006): 523–31. doi:10.1086/501497.
- [4] V. Baglin, J. Bojko, O. Grabner, B. Henrist, N. Hilleret, C. Scheuerlein, M. Taborelli, *The secondary electron yield of technical materials and its variation with surface treatments*, Proceedings of EPAC 2000, 26-30 June 2000, Austria Center, Vienna, pp. 217-221.